Electronic Supplementary Information (ESI) for Inorganic Chemistry Frontiers

Hydroxy Reduced Silver Nanoparticles on Ultrathin Boron Imidazolate Framework Nanosheet for Electrocatalytic CO_2 Reduction

Ping Shao[a,b], Luocai Yi[b], Jun-Qiang Chen[b], Changsheng Cao[b], Hai-Xia Zhang[b]* and Jian Zhang[b]*

[a]*College of Chemistry, Fuzhou University, Fuzhou, Fujian 350108, P. R. China.*

[b]*State Key Laboratory of Structural Chemistry, Fujian Institute of Research on the Structure of Matter, Chinese Academy of Sciences, Fuzhou, Fujian 350002, P. R. China.*

Email: zhanghaixia@fjirsm.ac.cn; zhj@fjirsm.ac.cn.

Contents

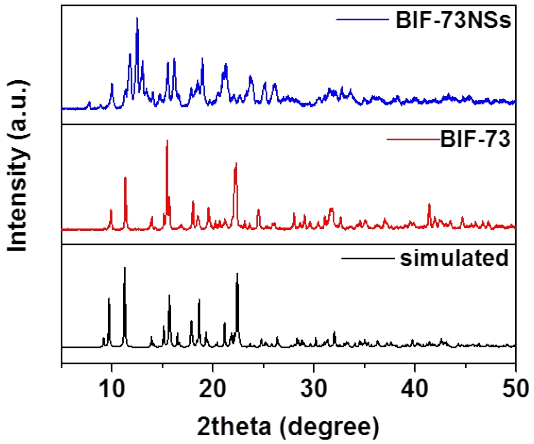

Figure S1. PXRD patterns of BIF-73, BIF-73NSs.

The diffraction peak of layered BIF-73NSs is consistent with that of BIF-73, only the peak intensity changed slightly, and the position of the diffraction peak at 10-15 degrees slightly changed. We hypothesize that these changes are due to the fact that the three $BH(im)_3^-$ (im = imidazolate) ligands of layered BIF-73NSs unit cell cannot be kept in the same plane or have been twisted after the bulk crystal is exfoliated into layered.

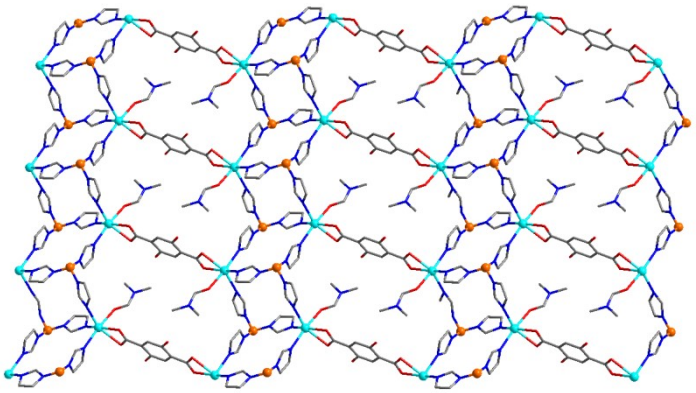

Figure S2. The 2,5-dihydroxyterephthalate ligands decorated 2D monolayer structure of BIF-73 crystal.

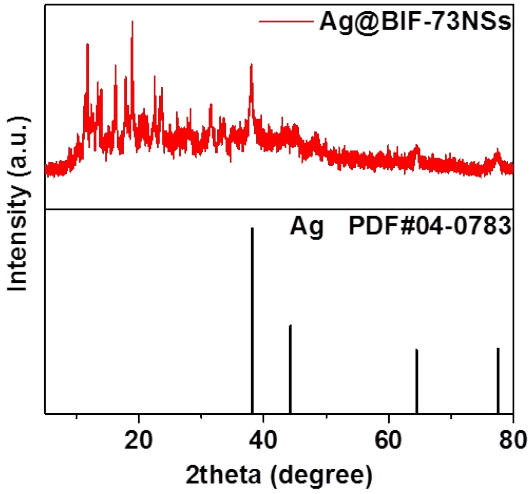

Figure S3. PXRD patterns of Ag@BIF-73NSs electrocatalysts.

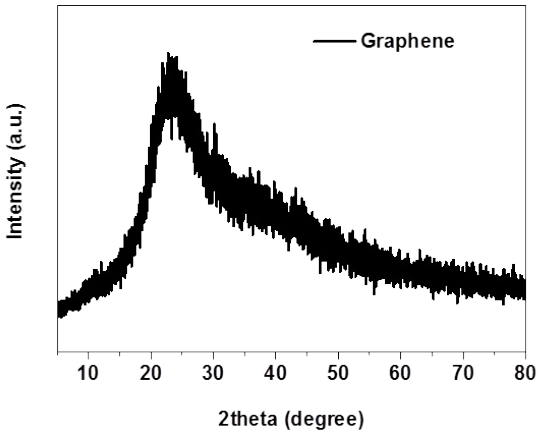

Figure S4. PXRD patterns of Graphene.

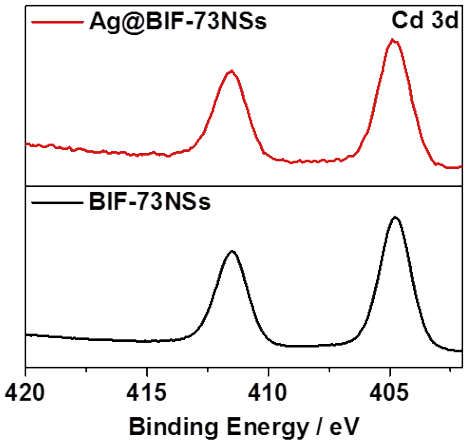

Figure S5. High-resolution Cd 3d XPS spectrum of Ag@BIF-73NSs, BIF-73NSs electrocatalysts.

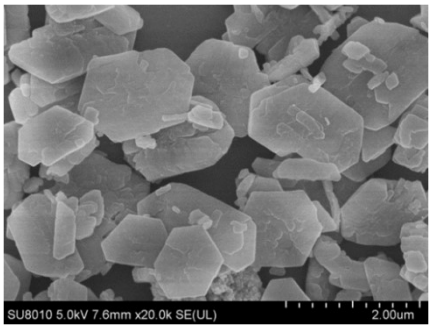

Figure S6. SEM images of BIF-73NSs electrocatalysts.

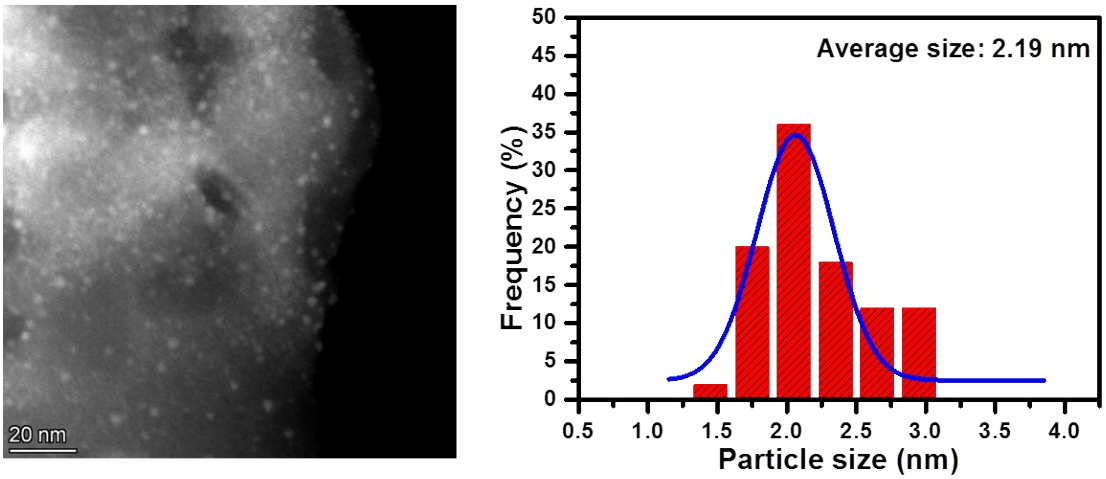

Figure S7. TEM images of Ag@BIF-73NSs electrocatalysts.

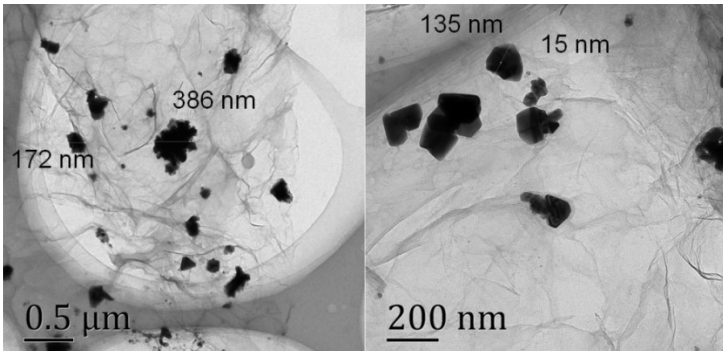

Figure S8. TEM images of Ag@Graphene electrocatalysts.

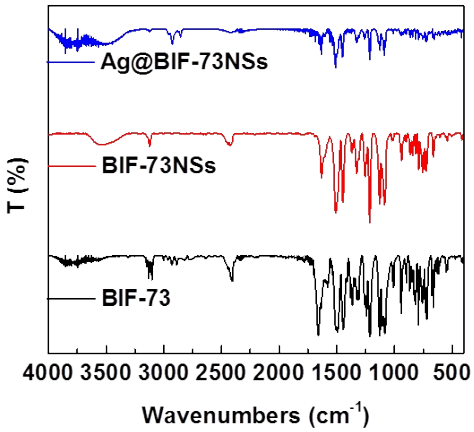

Figure S9. Infrared spectra for BIF-73, BIF-73NSs, and Ag@BIF-73NSs electrocatalysts.

FT-IR experiments display that the adsorption peaks located at 1100~1200 cm^{-1} weaken when introducing Ag^{+} into framework, and the adsorption peaks can be ascribed to the character adsorption of C-OH groups, suggesting that the Ag^{+} had interaction with functional -OH groups in the BIF-73.

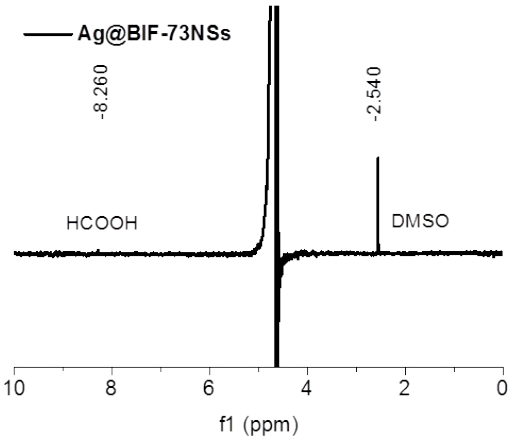

Figure S10. 1H NMR of the liquid products for Ag@BIF-73NSs after 1 h electrolysis.

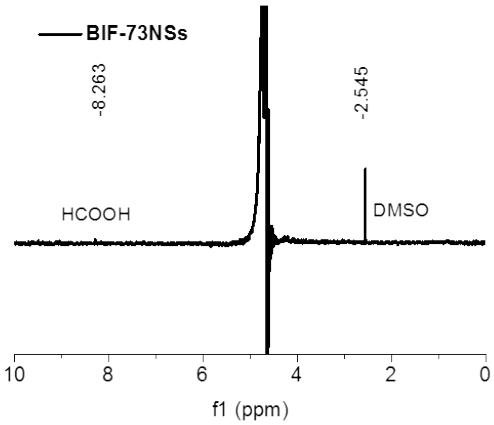

Figure S11. 1H NMR of the liquid products for BIF-73NSs after 1 h electrolysis.

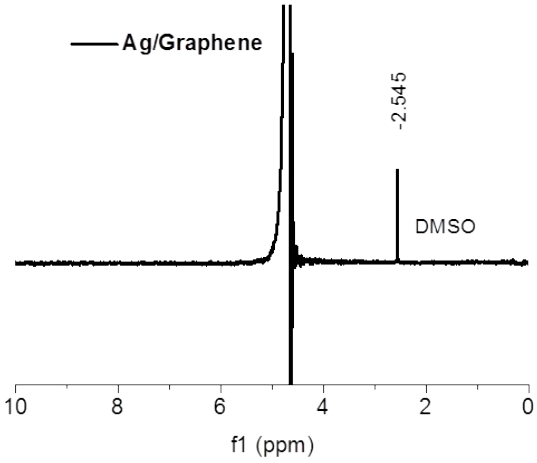

Figure S12. 1H NMR of the liquid products for Ag@Graphene after 1 h electrolysis.

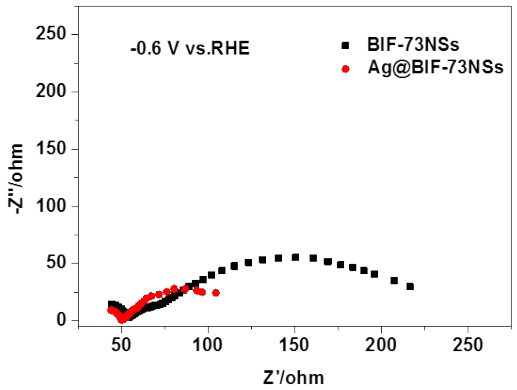

Figure S13. Nyquist plots of electrocatalysts over the frequency ranging from 100 kHz to 0.1 Hz at -0.6 V vs.RHE.

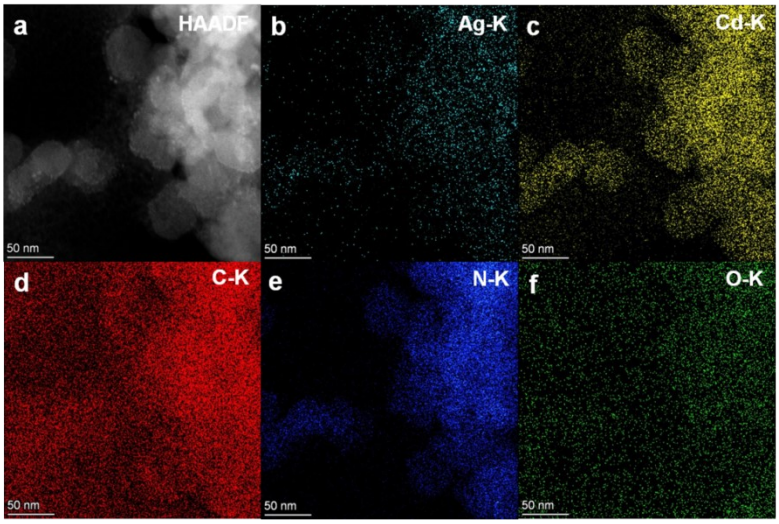

Figure S14. The morphology characterization of Ag@BIF-73NSs after electrocatalysis. a) STEM and b) Ag; c) Cd; d) C; e) N; f) O element mapping images.

To further investigate the stability of Ag@BIF-73NSs after CO_2RR, STEM and energy dispersive X-ray (EDX) elemental mapping tests have been conducted. EDX elemental mapping images show that Ag is uniformly distributed in Ag@BIF-73NSs after CO_2RR, suggesting the good stability of the Ag@BIF-73NSs after CO_2RR.

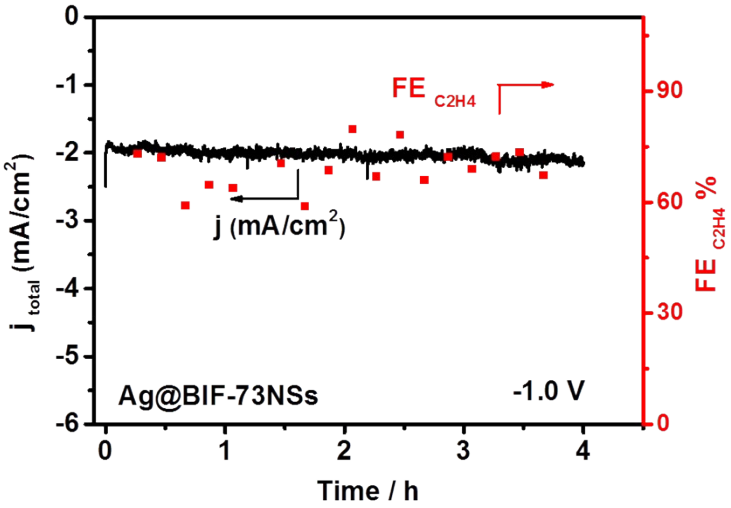

Figure S15. The total current density and FE of CO over 4 h electrolysis on Ag@BIF-73NSs catalysts at -1.0 V vs. RHE.

The electrochemistry durability test results reveal that the current density of Ag@BIF-73NSs indicates no significant decay for 4 h at ‒1.0 V versus RHE; moreover, the FE of CO keeps at ≈60%, implying the Ag@BIF-73NSs can maintain both the activity and selectivity during the CO_2 reduction process.